Electronic supplementary information (ESI)

Ultraviolet phototoxicity of upconversion nanoparticles illuminated with near-infrared light

K. E. Mironova,[a,b] D. A. Khochenkov,[a,c] A. N. Generalova,[a,b] V. V. Rocheva,[a] N. V. Sholina,[a,c] A. V. Nechaev,[a,d] V. A. Semchishen,[a] S. M. Deyev,†[b] A. V. Zvyagin,†[e,f] E. V. Khaydukov[d,e,a]

[a]Federal Scientific Research Centre "Crystallography and Photonics" of Russian Academy of Sciences, Leninsky pr. 59, Moscow, 119333, Russia.

[b]Shemyakin-Ovchinnikov Institute of Bioorganic Chemistry of the Russian Academy of Sciences, 16/10 Miklukho-Maklaya, Moscow 117997, Russia.

[c]FSBSI "N.N. Blokhin Russian Cancer Research Center" of Ministry of Health of the Russian Federation, 24 Kashirskoye shosse, Moscow, 115478, Russia.

[d]Institute of Fine Chemical Technologies, Moscow Technological University, 86 Prospect Vernadskogo, 119571 Moscow, Russia.

[e]Institute of Molecular Medicine, Sechenov First Moscow State Medical University, Trubetskaya 8, 119991 Moscow, Russia.

[f]ARC Centre of Excellence for Nanoscale BioPhotonics (CNBP), Macquarie University, Sydney, NSW 2109, Australia.

[d]International Joint Center for Biomedical Innovation, School of Life Sciences, Henan University, Kaifeng, Henan 475004, China

† Corresponding authors:

Andrey V. Zvyagin, E-mail: andrei.zvyagin@mq.edu.au;

Sergey M. Deyev E-mail: deyev@ibch.ru.

SI 1. Internalization of bioconjugates

Treated with DARPin-mCherry/UCNPs bioconjugates cells were analyzed in Stokes excitation/detection channel. mCherry in the bioconjugate and LysoTracker Green, staining acidic compartments, such as lysosomes in live cells, were utilized as a Stokes fluorescent label to confirm the bioconjugates internalization. The appearance of yellow color as a result of overlapping of LysoTracker's green and mCherry's red fluorescence pointed at the lysosomal localization of DARPin-mCherry/UCNP bioconjugates. After 2 hours of co-incubation at 37°C, significant overlapping of luminescent signals of DARPin-mCherry/UCNP conjugates and LysoTracker revealed the bright yellow dots, associated with the conjugate localization in acidic compartments (see Figure S1). Such scenario was the reason to assume that efficient receptor HER2/neu-mediated binding and internalization occurred.

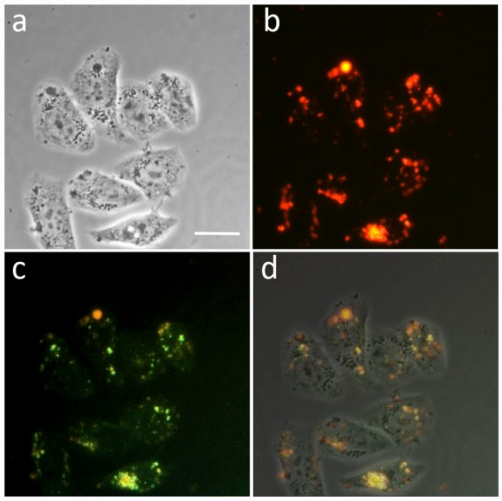

Figure S1. Intracellular localization of DARPin-mCherry/UCNPs bioconjugates. (a) Phase-contrast image of SK-BR-3 cells; (b) luminescence image of DARPin-mCherry/UCNPs (red detection channel); (c) lysosomes of SK-BR-3 stained with LysoTracker Green DND-26 (green detection channel); (d) overlapped images (yellow signal) of panels (a), (b) and (c). Scale bar, 20 μm.

Clathrin vesicles are known to be size-limited to 100 nm, while our as-synthesised nanoparticles (NPs) were sized 100×150nm. We also note that NPs sized <100 nm are reported to be internalised passively with concomitant cytotoxic effects comparing in comparison with NPs sized >100 nm [1-3]. Rejman, et al have shown that latex beads <200 nm and <500 nm in diameter were uptaken by non-phagocytic cells by the clathrin- and caveolae-mediated endocytosis, respectively [4]. In addition, viruses, such as HIV-1 120 nm in diameter and Rhadinovirus 150-200 nm in diameter, are known to enter cells by the clathrin-mediated endocytosis. This brief literature survey shows some ambiguity and knowledge gaps in our understanding of mechanisms of the clathrin-mediated endocytosis.

NP size, surface charge, cell type and experimental conditions influenced the NP cellular internalisation processes. Ligand density per nanoparticle represent one of the most important parameter, whereas the relatively small size of our reported recombinant protein DARPin-mCherry affords decoration of the UCNP surface at a high density. This is particularly important for HER2/neu receptors tending to cluster into "receptor clusters" of size 67 nm on the membrane [5]. Therefore, the number of NPs bound to the cell is determined by a number of such clusters, regardless of the

number of (overexpressed) receptors per cell, and hence the decoration of the UCNP surface with ligands at a high density represents a critical design parameter. To this aim, we showed that one UCNP hosted ~1000 of DARPin-Cherry molecules (see SI 8), meaning the ligand density was high indeed.

A new class of the synthetic non-immunoglobulin targeting ligands, DARPin, adds another dimension to the discussion of the possibility of the clathrin-medicated internalisation mechanism. Relatively low UCNP photoluminescent intensity in CHO cells (c.f. Fig. 3) and the lysosomal localisation of NPs in SKBR-3 cells pointed to the clathrin-mediated endocytosis as the main pathway of the UCNPs internalisation, although a micropinocytosis pathway cannot be excluded. At the same time, the mechanism of UCNP-DARPin-mCherry entry to target cells warrants further study.

SI 2. UV-phototoxicity of bioconjugates

Phase contrast and propidium iodide (PI) fluorescence images of SK-BR-3 cells incubated with UV-emitting DARPin-mCherry/UCNPs and NIR irradiated with 3500 J/cm^2 dose. The images were taken at different time (0, 60, 90 and 120 min) intervals after NIR PDT treatment.

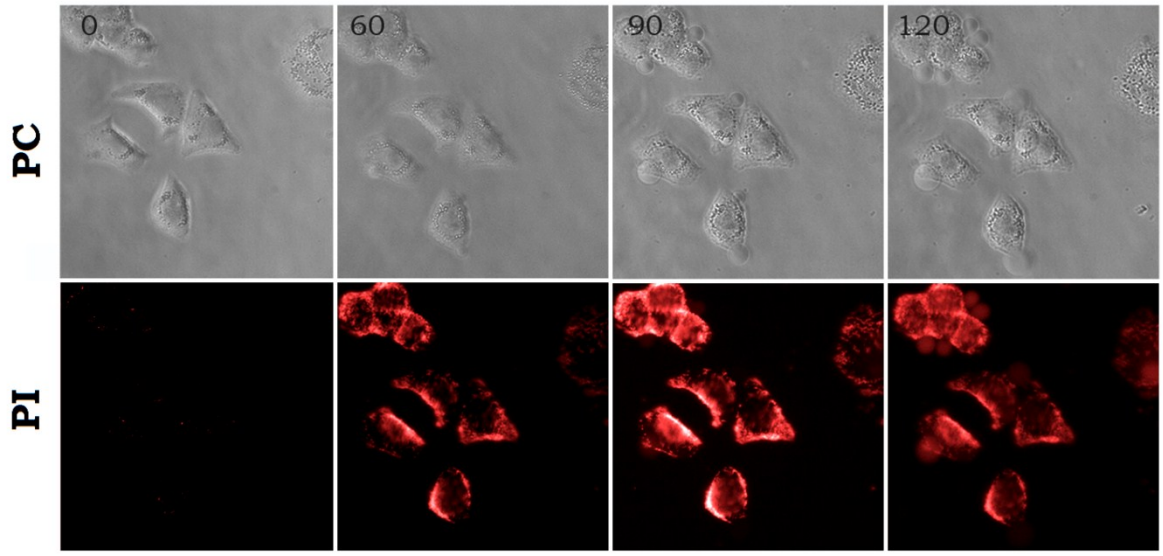

Figure S2. Manifestation of UV-phototoxicity of targeted DARPin-mCherry/UCNPs bioconjugates triggered by 975 nm laser light. (PC) Phase contrast and (PI) fluorescence images of SK-BR-3 cells stained with propidium iodide.

SI. 3. Evaluation of the cellular ROS production under UCNP bioconjugate photoactivation

To assess the mechanism of UCNP dependent phototoxicity, we performed an evaluation of the cytoplasmic ROS, using CellROX Deep Red (Molecular Probes/Thermo) – a fluorescent probe of cytoplasmic ROS. Briefly, SK-BR-3 cells (5×10^3) were seeded in 96-well plates and incubated with 2.5 µM of CellROX Deep Red and 2.5 µg DARPin-mCherry/UCNP conjugates in complete RPMI-1640 media with 10% FBS (Gibco) for 30 min and washed in PBS three times. Then 100-µL complete RPMI-1640 media without Phenol Red (Gibco) was added to cells and the plate was mounted in a fluorescent microscope (Motic, China) equipped with a semiconductor laser operating at a wavelength of 975 nm (ATC-SD, Russia) for cells irradiation. A cooled HR sCMOS camera (Photonic

Science, UK) was mounted on an optical port of the microscope. Cells were irradiated with the laser at a dose of 1200 J/cm^2. Optical images and CellROX fluorescence images of SK-BR-3 cells were acquired using a fluorescence cube with the excitation channel of 620/60 nm and emission channel of 700/75 nm to monitor the ROS induction. As a control, SK-BR-3 cells irradiated with 1200 J/cm^2 at 975 nm with "UV-free" UCNP were used (see Figure S3). According to the obtained data, UV-emitting UCNPs induced cytoplasmic ROS under 975 nm irradiation contrary to UV-free UCNP. This result support an assertion that the ROS-mediated mechanism was a prime contributor to the cell death resulting from our PDT treatment.

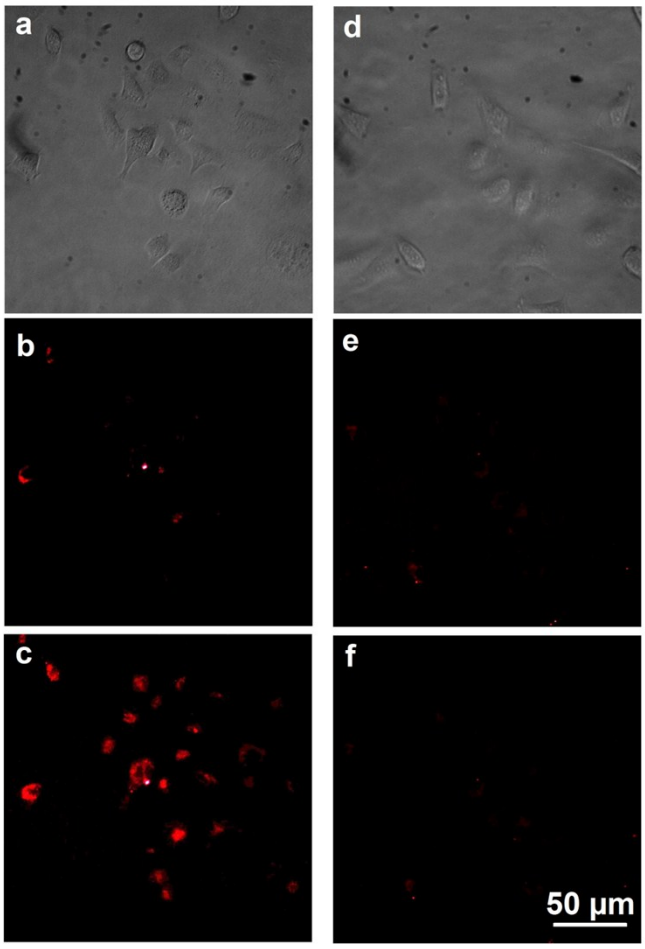

Figure S3. Observation of the cellular ROS production under DARPin-mCherry/UCNPs bioconjugates triggered by 975-nm laser light. (a) Phase contrast and (b,c) fluorescence images of SK-BR-3 cells stained with CellROX Deep Red and UV-emitting UCNPs, as compared to cells pre-incubated with UV-free UCNPs (d,e,f). (b) and (e) fluorescence images captured prior to the PDT treatment, (c) and (f) after the PDT treatment at a NIR light dose of 1200 J/cm^2. Strong fluorescent signal in (c) indicates the cellular ROS production in PDT with UV-emitting UCNPs.

SI 4. Temperature control

Distilled water heating in a well of 96-well plate under NIR irradiation with optical luminescent microscope was carried out. A micro-thermocouple (76 µm, Omega Engineering, USA) was employed for temperature control of a culture medium during the cell exposure to the laser irradiation,

including PDT procedure. The temperature was measured with micro thermocouple positioned into 150 µl of water.

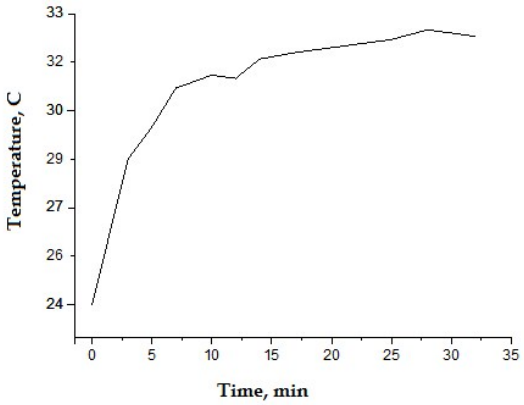

Figure S4. Distilled water heating in a well of 96-well plate under 975 nm pulse irradiation at average intensity 1.5 W/cm^2.

A diode laser (ATC-C4000-200-AMF-975, Semiconductor devices, Russia) operating at 975 nm in a pulse regime (pulse width 50 ms, repetition rate 8 Hz) was employed for *in vivo* PDT treatments. Laser light was coupled to a multimode optical fibre probe with a collimator for flexible delivery to tumour sites. Figure S5 shows the temperature distribution on the tumour surface after NIR irradiation at a dose of 1200 J/cm^2. A tumour site was irradiated in a raster-scanning regime, following UCNP peritumoural injection and incubation for 1.5 h. The tumour site temperature was monitored by means of an infrared camera (Gobi-384-GigE, Xenics, Belgium) to ensure safe physiological margins of the procedure (< 41 ^{o}C).

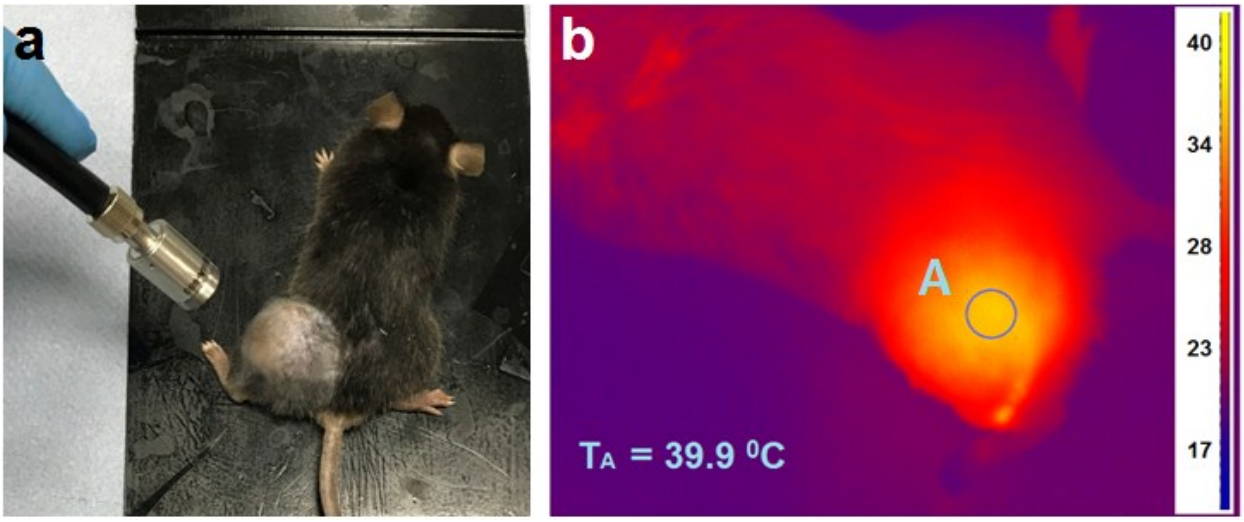

Figure S5. (a) An image and (b) pseudo-colour temperature map of a BDF_1 mouse with LLC tumor during a PDT treatment after NIR irradiation at a dose of 1200 J/cm^2. The temperature in the field labelled "A" did not exceeded the physiologically acceptable threshold of 40 ^{0}C.

SI 5. In vivo demonstration of UCNP UV-phototoxicity

In vivo NIR PDT treatment of tumor was perfomed on the inoculated model of epidermoid Lewis lung carcinoma (Lewis lung cancer, LLC, ATCC, CRL-1642™). Laboratory animals, which were treated at laser exposure without UCNPs injection, were used as a control group. Animals injected with β-$NaYF_4$: Yb^{3+}, Er^{3+}/$NaYF_4$ nanoparticles were called UV-free UCNP group, injected with β-$NaYF_4$: Yb^{3+}, Tm^{3+}/$NaYF_4$ – UV-emitting group. In figure S6 the tumor volume evolutions after NIR laser treatment (0 days) in three groups are shown.

Figure S6. Photographs of LLC bearing mice taken on the 3th and 14th days after NIR PDT treatment.

Figure S7 demonstrates the histological images of the tumor tissue sections stained with hematoxylin and eosin, excised 2 day after the 975-nm PDT treatment. UCNPs in PBS solution were injected peritumorally. UV-emitting UCNPs after irradiation display profound hemorrhages, respectively, whereas control and UV-free UCNPs shows no abnormalities.

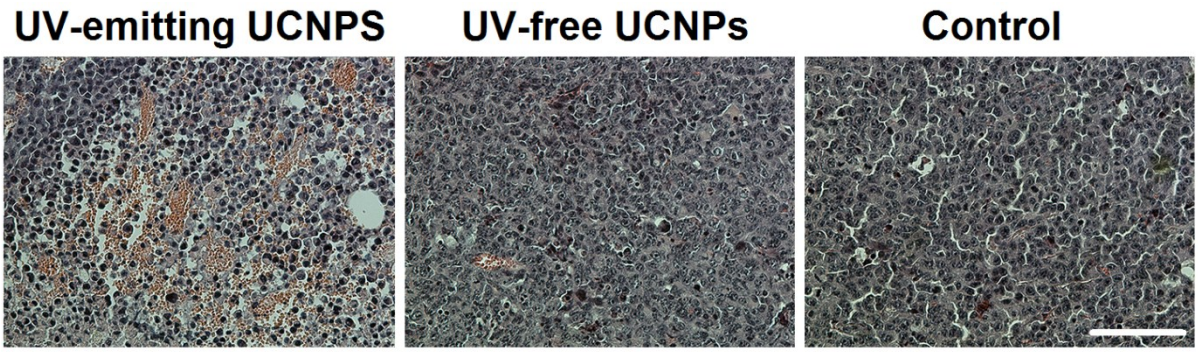

Figure S7. The histological tumor tissue images after haematoxylin and eosin (H&E) staining.

SI 6. UCNPs synthesis

The mixture of Y_2O_3 (0.794 mmol), Yb_2O_3 (0.2 mmol), Tm_2O_3 (0.06 mmol) was suspended in 10 ml 70% trifluoroacetic acid and gentle refluxed until a clear solution was obtained (≈ 6h), then cooled to room temperature. Solution was evaporated and residue was dried in vacuum (0.1 Torr) for 1h. This rare-earth trifluoroacetate mixture and sodium trifluoroacetate (2.5 mmol) were added to 10 ml oleic acid and 10 ml 1-octadecene in three-neck flask equipped the thermometer and glass magnetic stirrer. The solution was heated up to 120 °C and stirred under vacuum for 30 min for degassing and water removing. Then, the mixture was gradually heated at a rate of 200 °C/min to 320 °C on Wood's alloy bath and incubated at this temperature for 30 min in argon atmosphere. Then, the

mixture was cooled by adding 15 ml 1-octadecene. In order to cool to room temperature 150 ml propanol-2 was added and mixture was centrifuged at 6000 rpm for 20 min. Obtained nanocrystals were purified by absolute ethanol addition, dried, and dissolved in 10 ml oleic acid and 10 ml 1-octadecene. Yttrium trifluoroacetate (previously prepared from 0.5 mmol Y_2O_3 and 5 ml 70% CF_3COOH, as described above) and sodium trifluoroacetate (1 mmol) were added, mixture was heated up to 120 ^oC and stirred under vacuum for 30 min. Then, the mixture was heated up to 305 ^oC, incubated for 15 min on Wood's alloy bath in argon atmosphere and cooled to room temperature. Obtained core/shell nanoparticles were centrifuged at 6000 rpm for 20 min. The product of synthesis is hydrophobic monodisperse nanoparticles with a core/shell structure (β-$NaYF_4$:$Yb^{3+}Tm^{3+}$/$NaYF_4$) capable of forming stable colloids in non-polar organic solvents such as hexane and chloroform.

We used the UCNPs β-$NaYF_4$:$Yb^{3+}Er^{3+}$/$NaYF_4$ with green and red luminescent bands as a control of nanoparticles phototoxicity. UCNPs were synthesized with initial mixture of Y_2O_3 (0.78 mmol), Yb_2O_3 (0.2 mmol), Er_2O_3 (0.2 mmol) by the same method.

SI 7. UCNP cytotoxicity (MTT-assay)

Normal human foreskin fibroblast cells BJ-5ta were placed on 96-well plates (Nunc, Denmark), 5000 cells/well in complete RPMI-1640 media with 10% PBS and incubated for 24 h at 37 °C on 5% CO_2 atmosphere. PMAO-coated UCNPs were added to the wells at a concentration range of 6 to 100 μg/mL, NPs were sonicated for 10 min prior to the treatment. Intact cells with equal volumes of the culture medium were used as a control. After 48 h incubation with UCNPs a colorimetric MTT analysis was performed. The medium with particles was removed, cells were washed with PBS twice, replaced by fresh medium, and 20 μL/well of MTT (final concentration 0.5 mg/mL) were added and incubated for 4 h to precipitate insoluble purple crystals of formazan by mitochondrial succinate dehydrogenase of viable cells. The medium was then replaced with 200 μL/well DMSO to dissolve formed crystals. The colour intensity of the formazan solution reporting on the cell growth was measured at 540 nm using a Multiscan FC microplate analyzer (Thermo Scientific, USA). The cell survival was calculated by using the following formula:

$$(OD_{\text{experimental group}} - OD_{\text{control group}}) / OD_{\text{control group}} * 100\%,$$

where OD stands for the optical density of assayed solution.

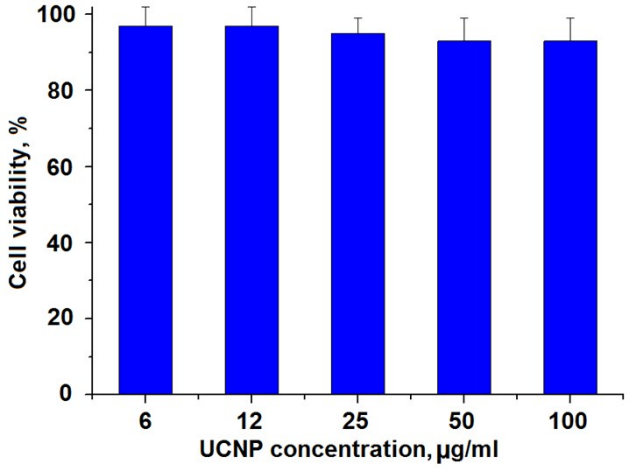

Figure S8. A histogram of the cell viability using MTT assay. BJ-5ta cell line was treated with PMAO-coated UCNPs. Nanoparticles impart negligible stress on cells ranged from 93 to 98%, showing no statistical significance in the cell viability.

SI 8. Estimation of DARPin-mCherry molecule concentration on the UCNP surface

The photoluminescent (PL) spectrum of DARPin-mCherry/UCNPs bioconjugates under 543 nm excitation are shown in fig. S9.

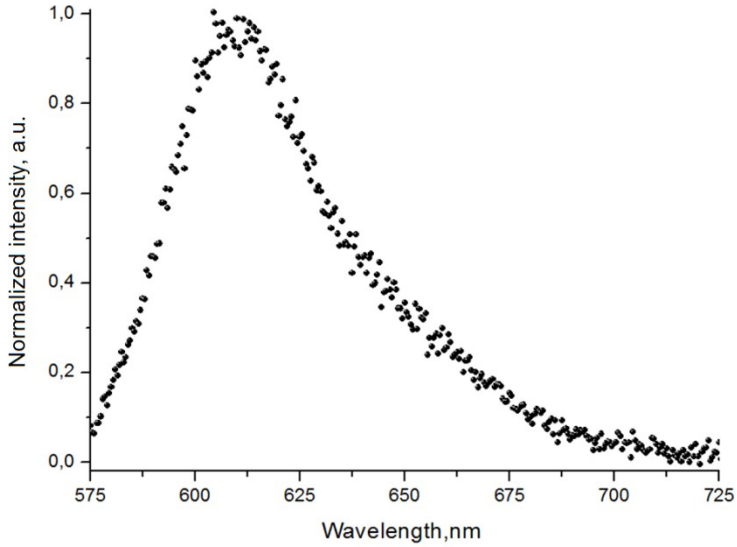

Figure S9. Photoluminescent spectrum of DARPin-mCherry/UCNP bioconjugates under 543 nm excitation.

The concentration of DARPin-mCherry molecules was determined as $\nu = 6.7 \times 10^{-7}$ M by analysing the PL spectrum and benchmarking it against UCNP-free calibration sample. UCNP concentration in the sample was C_{ucnp}=0.3 mg/mL. The nanoparticle density was found in [6]: ρ= 4.2 g/cm^3.

The mass of a single nanoparticle is estimated as:

$M_{ucnp} = V \times \rho = 7.56 \times 10^{-15}$ g, where V is the volume of nanoparticle.

Then, the quantity of DARPin-mCherry molecules on the surface of the single UCNP is found as

$$N = \frac{\nu \times N_a \times M_{UCNP}}{C_{UCNP}} \approx 1000$$

,

where N_a is Avogadro's number.

SI 9. UCNP conversion efficiency

The conversion efficiency η_{uc} measurements were performed using a calibrated integrating sphere setup, as described by us previously [7]. UCNPs powder to be measured was placed in a sample holder and illuminated by a 975-nm laser light through an entrance port of the integrating sphere. Using appropriate filters to account for the UCNP spectrum and a photodiode placed at a perpendicular exit port of the sphere, both emitted P_{em} and absorbed P_{abs} powers were measured over a range of the excitation intensities. η_{uc} was calculated using the definition of P_{em}/P_{abs} [W/W]*100%.

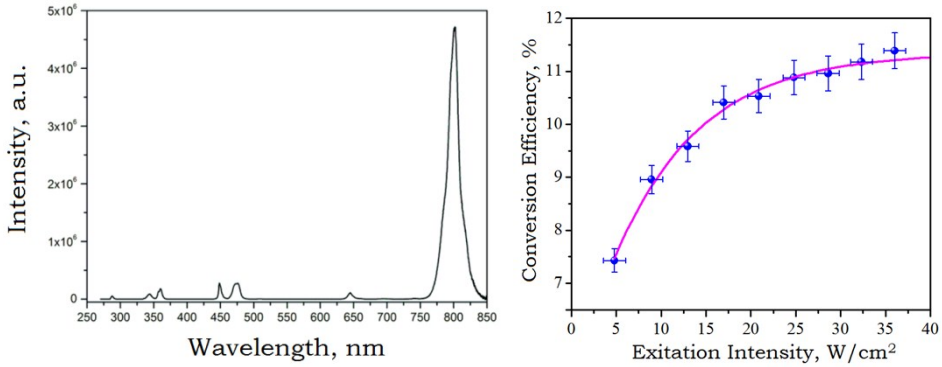

Figure S10. Full emission spectrum of the β-$NaYF_4$:$Yb^{3+}Tm^{3+}$/$NaYF_4$ UCNPs powder with the excitation by a 975-nm laser at the intensity value of 5 W/cm². Absolute conversion efficiency of UCNPs versus the excitation intensity at 975 nm measured using the calibrated integrating sphere setup.

An emission spectrum of the β-$NaYF_4$:$Yb^{3+}Tm^{3+}$/$NaYF_4$ UCNPs powder was acquired using a calibrated fluorimeter (Fluorolog-3, Horiba JY, France) with excitation by a 975-nm laser at the intensity 5 W/cm², and is shown in Figure S10. The spectrum featured five emission bands, which are known to result from the Tm^{3+} electronic transitions.

References

1. Jiang X, et al. Endoand exocytosis of zwitterionic quantum dot nanoparticles by live HeLa cells. ACS Nano, 2010, 4:6787–6797.

2. Yang L, et al. Mechanistic aspects of fluorescent gold nanocluster internalization by live HeLa cells. Nanoscale, 2013, 5:1537–1543.

3. Shang L, et al. Intracellular thermometry by using fluorescent gold nanoclusters. Angew Chem Int Ed Engl, 2013, 52:11154–11157.

4. Rejman J, et al. Size-dependent internalization of particles via the pathways of clathrin- and caveolae-mediated endocytosis. Biochem J, 2004, 377:159–169.

5. Kaufmann R, et al. Analysis of Her2/neu membrane protein clusters in different types of breast cancer cells using localization microscopy. J Microsc, 2011, 242: 46-54.

6. Liu H, et al. Deep tissue optical imaging of upconverting nanoparticles enabled by exploiting higher intrinsic quantum yield through use of millisecond single pulse excitation with high peak power. Nanoscale, 2013, 5, 10034–10040.

7. Grebenik E, et al. Feasibility study of the optical imaging of a breast cancer lesion labeled with upconversion nanoparticle biocomplexes. J Biomed Opt, 2013, 18:76004.